IOP Publishing Journal of Physics: Condensed Matter
J. Phys.: Condens. Matter **32** (2020) 165502 (6pp) https://doi.org/10.1088/1361-648X/ab6740

Physical mechanisms for the optical properties of the femtosecond-laser-treated black diamond

Xiao Dong[1,2,3], **Yongyong Wang**[1,2] **and Xiaohui Song**[1,2]

[1] School of Physics, Henan Normal University, 453007 Xinxiang, People's Republic of China
[2] Henan Key Laboratory of Photovoltaic Materials, 453007 Xinxiang, People's Republic of China

E-mail: dongxiaosmall301@163.com

Received 23 September 2019, revised 30 November 2019
Accepted for publication 3 January 2020
Published 23 January 2020

Abstract

Vacancies in diamond can introduce defect bands in the band gap of diamond and lead to the sub-band gap absorption in the visible and infrared regions. At sufficiently high concentrations of vacancy, the defect bands overlap each other to form a single partially filled intermediate band (IB) in the band gap and the sub-band gap absorption in the infrared region is especially strong. Along with the decreasing of the vacancy concentrations, the IB splits into two separate bands and the sub-band gap absorption decreases sharply. The computed results are important for thoroughly understanding of the optical properties of black diamond.

Keywords: intermediate band, black diamond, sub-band gap absorption, first-principles calculations

(Some figures may appear in colour only in the online journal)

1. Introduction

Chemical vapor deposition (CVD) diamond has attracted great interests due to its remarkable electronic characteristics such as high breakdown field, low dielectric constant, low leakage current, high carrier saturation velocity, and high carrier mobility [1–5]. These unique properties of diamond make it suitable for a wide range of applications in electronic devices, such as high-energy detectors, efficient thermionic converters, and so on [3–11]. Nevertheless, due to the wide band gap of the diamond (5.47 eV), it is transparent to sunlight which is mainly distributed in the visible and nearly infrared regions [4, 5]. Extending the photon absorption and response range of the diamond from the ultraviolet to the visible and infrared will further extend the applications of diamond in optoelectronic field, and it has great potential to develop and study.

Recently, researchers effectively improved the properties of the diamond by using femtosecond-laser-nanotextured method [4, 5, 12–16], i.e. irradiating the diamond film with high-intensity femtosecond laser pulses. After the femtosecond laser irradiation, a nanotextured surface is formed and it is called 'black diamond' due to its black appearance. The results indicate that the black diamond exhibits a significant enhancement of absorption in the visible and near-infrared regions, and that the absorption depends on the laser parameters, e.g. laser fluences and wavelengths [4, 5, 12–16]. In addition, the responsivity of the black diamond prepared under optimal parameter can be also enhanced in the visible and near-infrared regions [4, 12, 16]. These properties would make the black diamond the most promising material for photo-enhanced thermionic emission (PETE) cathodes, which is a newly proposed solar energy conversion mechanism and could make the conversion efficiency reach 56% [15–18]. Nevertheless, compared with the excellent absorption for solar energy, the responsivity of the black diamond is still weak, which is unable to meet the desired requirements in actual applications.

To improve the responsivity of the black diamond in the solar spectrum, we first need to thoroughly understand the physical mechanisms of the optical and electrical properties of the material. Up to now, although researchers attribute the sub-band gap absorption and responsivity of the black diamond to the introduction of energy levels/bands in the band gap [4, 12, 13, 16], the relevant theoretical researches are scarce and the

[3] Author to whom any correspondence should be addressed.

features of the energy levels/bands are unknown. In this work, to further understand the physical mechanisms of the properties of the black diamond, and then optimize its optoelectronic characteristic, we study the properties of the material based on first-principles calculations. We first construct several probable configurations of intrinsic defects in the diamond, and then calculate their electronic structures and optical properties. By comparing the computed results with the experimental ones, we can speculate the dominant defects exist in the black diamond and explain the properties of the material.

2. Computational methods

All the calculations are performed by using the density function theory (DFT) in the CASTEP code of Materials Studio [19–21]. The core electrons are represented by the ultrasoft pseudo-potential calculations, and the exchange-correlation potential is described by the Perdew–Burke–Ernzerhof (PBE) functional of generalized gradient approximation (GGA) [22, 23]. The geometry optimizations are performed by the Broyden, Fletcher, Goldfarb, and Shanno (BFGS) algorithm [24]. The plane-wave energy cutoff established for the basis set is 380 eV for all of the configurations. In order to investigate the effects of defect concentrations on the properties of the material, we construct supercells with various sizes and all of the supercells in this work are based on the conventional C_8 cubic cell. For the $2 \times 2 \times 2$ and $2 \times 2 \times 3$ supercells, the k-points sampling are set as $3 \times 3 \times 3$ for geometry optimization, while for the $2 \times 3 \times 3$ and $3 \times 3 \times 3$ supercells, the k-points sampling are set at $2 \times 2 \times 2$ for geometry optimization. The convergence tolerances in geometry optimization are set as follows: the total energy is set at 1×10^{-5} eV/atom, the maximum force is set at 0.03 eV Å^{-1}, the maximum stress is set at 0.05 GPa, and the displacement is set at 0.001 Å. The self-consistent field (SCF) tolerance to optimize the electronic structure is set at 1×10^{-6} eV/atom. The optical absorption properties are investigated by calculating the imaginary parts of the dielectric functions, which are obtained from the momentum matrix elements between the occupied and unoccupied wave functions with proper selection rules [25].

3. Results and discussion

According to the preparation process of black diamond in experiment [4, 5, 12–16], we speculate that the enhancement of the absorptance of diamond after treating by femtosecond laser pulses should be essentially due to the introduction of intrinsic defects of diamond. Nevertheless, the formation process of defects in the black diamond should be different from that in the conventional diamond. For the femtosecond-laser-treated black diamond, the formation mechanism of the surface texture should be the same as that of the black silicon: the strong interaction between femtosecond laser and the semiconductor surface results directly in a solid-vapor transition, which is a non-thermal ablation process [26, 27]. Therefore, the formation process of defects is a highly non-equilibrium process, and the formation energy would not play a key role in determining the dominant defects in the material [28]. Based on these results, we first construct several probable configurations of the intrinsic defects, such as vacancy and self-interstitial configurations, which are shown in figure 1. For the vacancy configuration, we just remove one of the C atom in the crystalline diamond supercell (figure 1(a)). For the self-interstitial configurations, we find that the three-bonds self-interstitial (figure 1(b)) and four-bonds self-interstitial configurations (figure 1(c)) are the most probable ones. For the other self-interstitial configurations, such as bond-center, hexagonal, and tetrahedral configurations, they can easily transform into the three-bonds or four-bonds ones in the process of geometry optimization. In the three-bonds self-interstitial configuration, the C-C bond lengths between self-interstitial C atom and other three C atoms are 1.42, 1.42, and 1.29 Å, respectively, shorter than the C–C bond length in perfect diamond crystal (1.54 Å). In the four-bonds self-interstitial configuration, the C–C bond lengths are 1.42, 1.42, 1.51, and 1.51 Å, respectively. Figure 1(d) shows the imaginary parts of the dielectric functions of the three intrinsic defect configurations in $2 \times 2 \times 2$ supercell, together with that of the perfect diamond crystal. The results indicate that the optical properties of the three-bonds and four-bonds self-interstitial configurations are similar to that of the perfect crystalline diamond, which can barely absorb the photons with energies less than about 5 eV. As for the vacancy configuration, it exhibits an extremely strong sub-band gap absorption for the photons with energies less than 0.7 eV (infrared region) and a relatively weak absorption at the photon energies from 2.2 to 3.1 eV (visible region). Based on these computed results, we can conclude that the enhanced absorption of the femtosecond-laser textured diamond in visible and near-infrared regions should be essentially attributed to the contribution of vacancy defects after femtosecond-laser irradiation. In addition, the sub-band gap absorption can be further enhanced by the multiple reflections from the surface periodic nanotexture of the black diamond.

To further investigate the mechanisms of the sub-band gap absorption induced by the vacancies, we then calculate the electronic structures of the vacancies at different concentrations. Figure 2 shows the total and partial density of states (DOS) of the vacancies in $2 \times 1 \times 1$, $2 \times 2 \times 1$, $2 \times 2 \times 2$, $2 \times 2 \times 3$, $2 \times 3 \times 3$, and $3 \times 3 \times 3$ supercells, respectively. The vacancy concentrations are 6.3%, 3.1%, 1.6 %, 1%, 0.69%, and 0.46%, respectively. For comparison, the total and partial DOS of the perfect crystalline diamond are also provided. The computed band gap of the perfect crystalline diamond is 4.54 eV, lower than the experimental value (5.47 eV) [4, 5], which is due to the well-known underestimation of the semiconductor band gap calculated by the GGA method. The total DOS results indicate that the vacancy at a wide range of concentrations can introduce intermediate bands (IB) in the band gap of diamond. From the partial DOS results, it can be found clearly that the IB in the band gap is mainly contributed by the p states of C atoms. At the low vacancy concentrations, such as 0.69% and 0.46%, the IB consists of two separate narrow bands. The upper band is empty while the lower one is almost filled by electrons. The two bands in the band gap

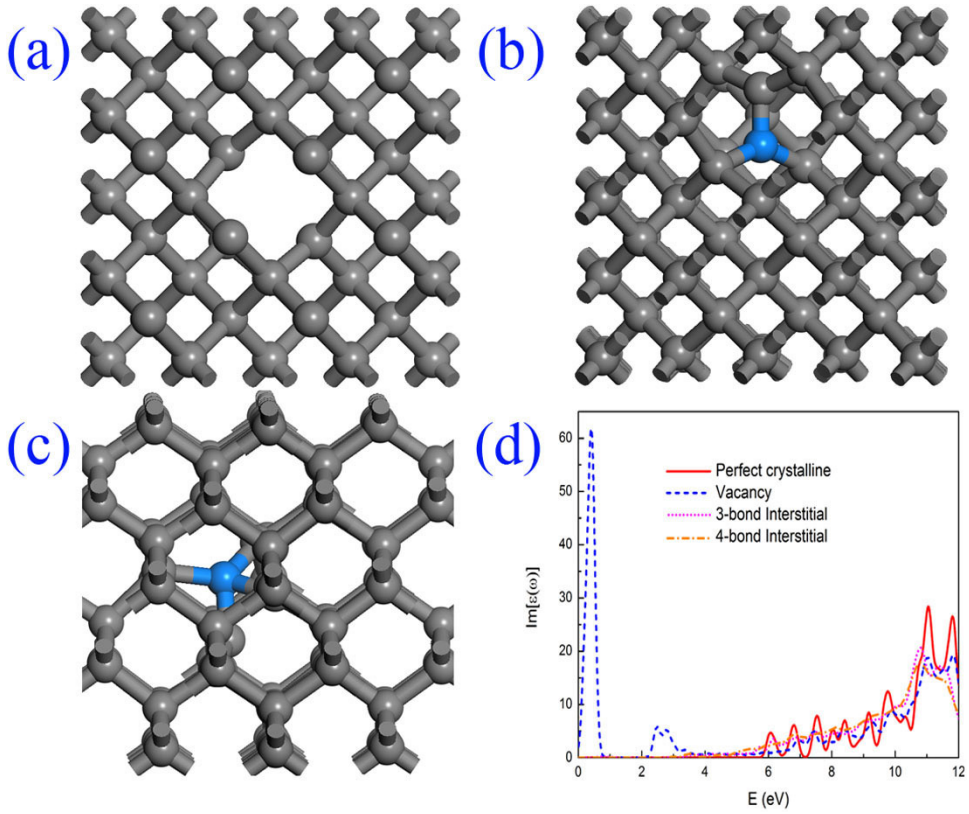

Figure 1. (a) Vacancy configuration in diamond; (b) three-bonds self-interstitial configuration in diamond; (c) four-bonds self-interstitial configuration in diamond; (d) imaginary parts of the dielectric functions of the three intrinsic defects configurations and perfect crystalline diamond. Blue balls represent the self-interstitial C atoms.

gradually come close to each other with the increasing of the vacancy concentration. When the concentration of vacancy is above 1%, the two defect bands overlap each other to form an IB which is partially filled with electrons. In this case, the electrons can be transfered from the valence band (VB) to the IB and from the IB to the conduction band (CB), together with the electrons transition in the IB. Nevertheless, at the excessive high concentration (6.3%), the IB disappears and the band gap reduces. The details of the electronic structures for the various supercells are listed in table 1. Therefore, we can find that the strong absorption in low energy (below 0.7 eV) for the $2 \times 2 \times 2$ supercell is due to the transition of electrons in the IB, and the weaker absorption peak at around 2.5 eV is due to the combined contribution of the transitions of electrons from the VB to the IB and from the IB to the CB. From table 1, it can be clearly found that with the increasing of the vacancy concentration, the energy difference between the VB maximum and the CB minimum increases (except the excessive high concentration). In addition, the energy differences from the VB maximum to the IB minimum and from the IB maximum to the CB minimum also nearly increase with the increasing of the vacancy concentration. Based on these results, it is hopeful to modulate the electronic structure of the black diamond by controlling the amount of vacancies which should be related to the laser parameters.

Figure 3 shows the optical properties of the configurations with various vacancy concentrations, which are investigated by calculating the imaginary parts of the dielectric functions. Consistent with the electronic structural results, the configurations with higher vacancy concentrations (smaller supercells) can lead to a strong absorption in the infrared region (below 0.7 eV), which is attributed to the transition of electrons in the partially filled IB. Nevertheless, the absorption in the infrared region reduces sharply with the decreasing of vacancy concentration, which is ascribed to the splitting of the IB. As an overall trend, the sub-band gap absorption for both of the infrared and visible regions increases along with the concentration of vacancy. Based on these computed results, we can give a reasonable interpretation for the relationship between the absorptance and the laser treatment dose in experiment. From the experimental researches, the increasing of the femtosecond laser dose can make the diamond textures become large [4, 15, 16]. Considering the intense interaction process between ultrafast laser pulses and diamond surface, the content of the intrinsic defects in diamond should increase with the enlargement of the textures or laser dose. The enlargement of the surface textures can lead to a better anti-reflection effect and the increasing of the intrinsic defects can lead to a strong sub-band gap absorption. Therefore, the increasing of the sub-band gap absorptance along with the increasing of the laser treatment dose should be due to the combined effects of the enlargement of the surface textures and the increasing of intrinsic defects of diamond, such as vacancies, which can introduce IBs in the band gap and lead to strong sub-band gap absorption. It should be noted that the computed optical properties based on the DFT calculations are only approximate and

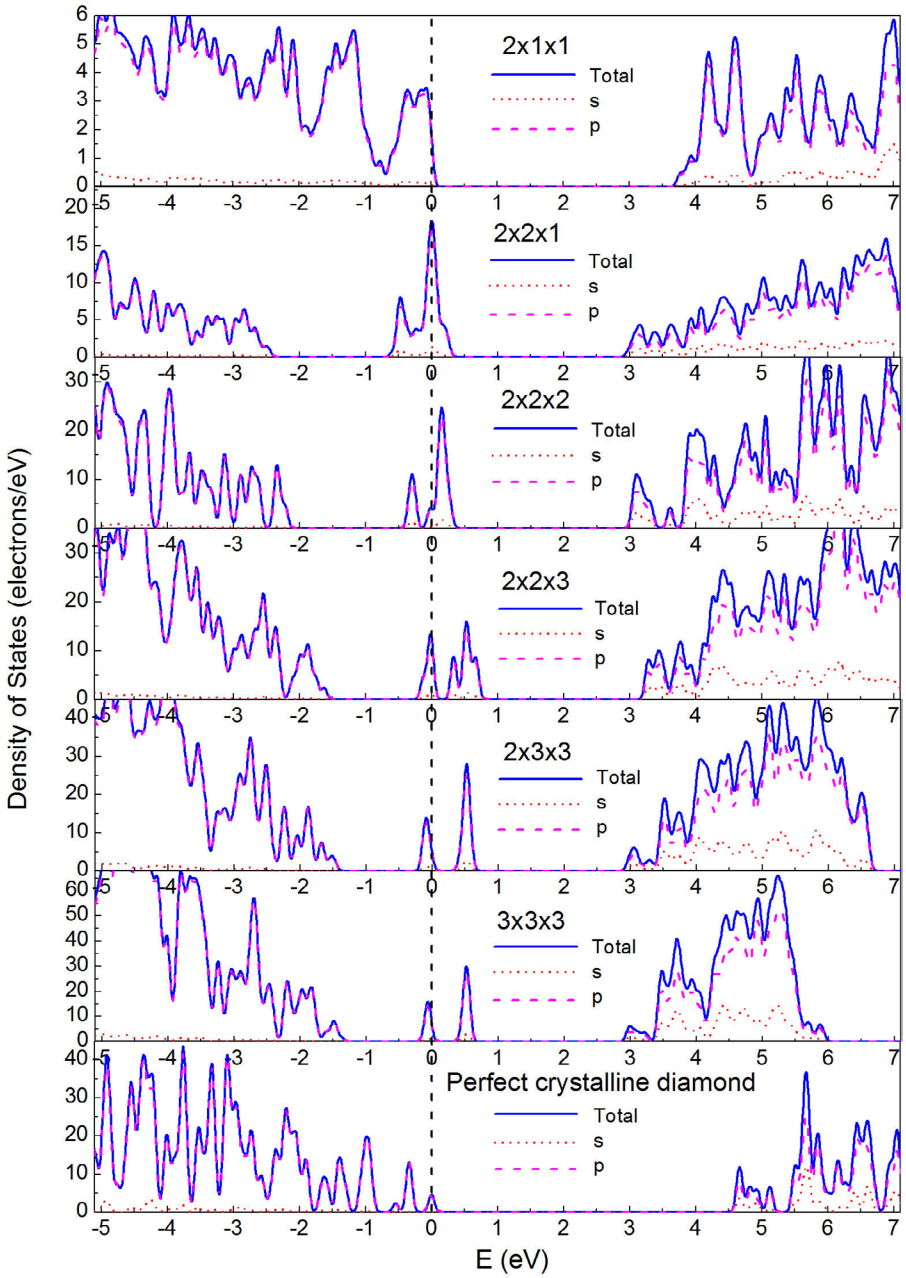

Figure 2. Total and partial density of states (DOS) of the perfect crystalline diamond and the vacancy configurations in $2 \times 1 \times 1$, $2 \times 2 \times 1$, $2 \times 2 \times 2$, $2 \times 2 \times 3$, $2 \times 3 \times 3$, and $3 \times 3 \times 3$ supercells, respectively.

Table 1. Electronic structural information of the vacancy configurations in different supercells. The values of electronic structural information are given in eV.

Supercell	Concentration	δE[VB-CB]	δE[VB-IB]	δE[IB-CB]
$2 \times 1 \times 1$	6.3%	3.56		
$2 \times 2 \times 1$	3.1%	5.25	1.72	2.54
$2 \times 2 \times 2$	1.6 %	5.06	1.67	2.58
$2 \times 2 \times 3$	1%	4.68	1.31	2.35
$2 \times 3 \times 3$	0.69%	4.25	1.15	2.22
$3 \times 3 \times 3$	0.46%	4.17	1.09	2.21

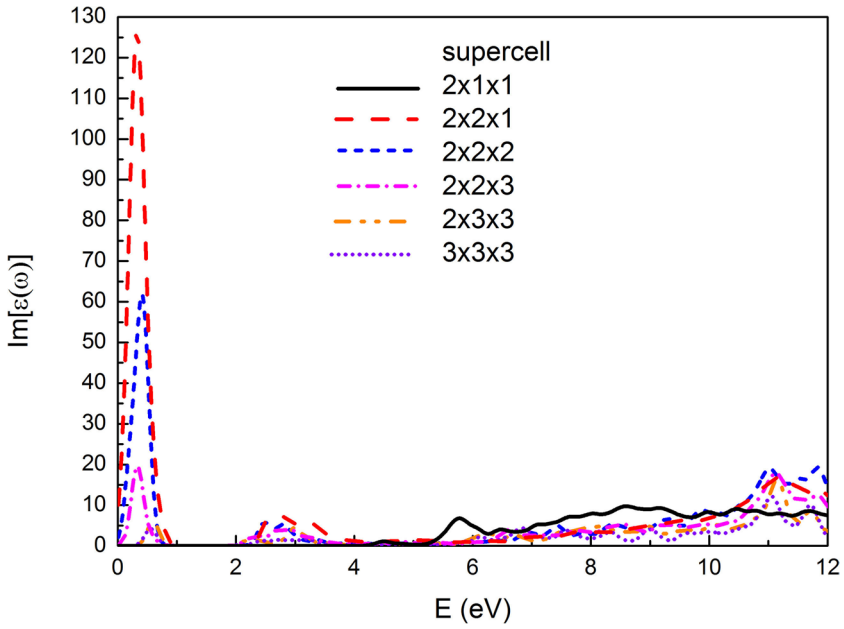

Figure 3. Imaginary parts of the dielectric functions of the vacancy configurations in $2 \times 1 \times 1$, $2 \times 2 \times 1$, $2 \times 2 \times 2$, $2 \times 2 \times 3$, $2 \times 3 \times 3$, and $3 \times 3 \times 3$ supercells, respectively.

some of the details may not be shown. Even so, the computed results can qualitatively reflect sub-band gap absorption of the black diamond and would not affect the conclusions of this study.

4. Conclusions

In summary, for the femtosecond-laser-treated black diamond, the unique strong absorption in the visible and infrared regions is due to the introduction of vacancies in the diamond during the ultrafast-laser irradiating process. The computed results indicate that the vacancies in diamond can introduce defect bands in the band gap of diamond and lead to the sub-bangap absorption in the visible and infrared regions. At high vacancy concentrations (except the excessive high concentration), the sub-band gap absorption in the infrared region is especially strong. Nevertheless, the infrared absorption reduces sharply as the vacancy concentration decreases. The absorption in the visible region also increases along with the increasing of the vacancy concentration. Our computed results can provide a reasonable explanation for the experimental phenomenon that the sub-band gap absorptance increases along with the laser treatment dose: the increasing of treatment dose would lead to the increasing of the vacancies which can introduce IBs in the band gap and enlarge the surface textures which can lead to a better anti-reflection effect. Therefore, how to improve the content of vacancies and inhibit the other kinds of defects is the key to optimize the properties of black diamond and needs to be studied further.

Acknowledgments

This work was supported by the National Natural Science Foundation of China (NSFC) under Grant Nos. 11804083 and the Youth Scientific Funds of Henan Normal University under Grant No. 2016QK05.

ORCID iDs

Xiao Dong https://orcid.org/0000-0003-3491-8058

References

[1] Balmer R S *et al* 2009 *J. Phys.: Condens. Matter* **21** 364221
[2] Calvani P *et al* 2009 *Diamond Relat. Mater.* **18** 786–8
[3] Conte G, Giovine E, Girolami M, Salvatori S, Bolshakov A, Ralchenko V and Konov V 2012 *Nanotechnology* **23** 075202
[4] Calvani P, Bellucci A, Girolami M, Orlando S, Valentini V, Polini R and Trucchi D M 2016 *Carbon* **105** 401–7
[5] Calvani P, Bellucci A, Girolami M, Orlando S, Valentini V, Polini R, Mezzetti A, Di Fonzo F and Trucchi D M 2016 *Appl. Phys.* A **122** 211
[6] Pomorski M, Caylar B and Bergonzo P 2013 *Appl. Phys. Lett.* **103** 112106
[7] Marinelli M, Milani E, Prestopino G, Scoccia M, Tucciarone A and Verona-Rinati G 2006 *Appl. Phys. Lett.* **89** 143509
[8] Girolami M *et al* 2017 *Carbon* **111** 48–53
[9] Rameau J D, Smedley J, Muller E M, Kidd T E and Johnson P D 2011 *Phys. Rev. Lett.* **106** 137602
[10] Lagomarsino S, Bellini M, Corsi C, Gorelli F, Parrini G, Santoro M and Sciortino S 2013 *Appl. Phys. Lett.* **103** 233507
[11] Caylar B, Pomorski M and Bergonzo P 2013 *Appl. Phys. Lett.* **103** 043504
[12] Bellucci A, Calvani P, Girolami M, Orlando S, Polini R and Trucchi D M 2016 *Appl. Surf. Sci.* **380** 8–11
[13] Girolami M, Bellucci A, Mastellone M, Orlando S, Valentini V, Montereali R M, Vincenti M A, Polini R and Trucchi D M 2018 *Carbon* **138** 384–9
[14] Calvani P, Bellucci A, Girolami M, Orlando S, Valentini V, Lettino A and Trucchi D M 2014 *Appl. Phys.* A **117** 25–9

[15] Calvani P, Bellucci A, Girolami M, Orlando S, Valentini V, Polini R and Trucchi D M 2015 *Phys. Status Solidi* a **212** 2463–7
[16] Girolami M, Bellucci A, Mastellone M, Orlando S, Valentini V, Montereali R M, Vincenti M A, Polini R and Trucchi D M 2017 *Phys. Status Solidi* a **214** 1700250
[17] Schwede J W *et al* 2010 *Nat. Mater.* **9** 762–7
[18] Segev G, Rosenwaks Y and Kribus A 2015 *Sol. Energ. Mat. Sol. Cells* **140** 464–76
[19] Hohenberg P and Kohn W 1964 *Phys. Rev.* **136** B864–71
[20] Kohn W and Sham L J 1965 *Phys. Rev.* **140** A1133–8
[21] Segall M D, Lindan P J D, Probert M J, Pickard C J, Hasnip P J, Clarke S J and Payne M C 2002 *J. Phys.: Condens. Matter* **14** 2717–44
[22] Vanderbilt D 1990 *Phys. Rev.* B **41** 7892–5
[23] Perdew J P, Burke K and Ernzerhof M 1996 *Phys. Rev. Lett.* **77** 3865–8
[24] Pfrommer B G, Côté M, Louie S G and Cohen M L 1997 *J. Comput. Phys.* **131** 233–40
[25] Sun J, Zhou X, Fan Y, Chen J and Wang H 2006 *Phys. Rev.* B **73** 045108
[26] Dong X, Li N, Shao H, Rong X, Liang C, Sun H, Feng G, Zhao L and Zhuang J 2014 *Appl. Phys. Lett.* **104** 091907
[27] Zhu J, Yin G, Zhao M, Ying D and Zhao L 2005 *Appl. Surf. Sci.* **245** 102–8
[28] Zhu Z, Shao H, Dong X, Li N, Ning B, Ning X, Zhao L and Zhuang J 2015 *Sci. Rep.* **5** 10513